European Journal of Clinical Pharmacy
Print ISSN: 2385-409X **Online ISSN**: 3105-0409
Website: https://farmclin.com/

Original Research Article

Synthesis and Characterizations Schiff Base New and Use it as Antagonists Antibacteria

Article History:

Name of Author:
Ali Faris Al-Ghezi[1] and Taghried A. Salman[2]

Affiliation:[1]*Department of Chemistry, College of Science, Al-Nahrain University, and A. Lect. In Iraqi ministry of Education, Thi Qar, 64016, Iraq.*
[2]*Department of Chemistry, College of Science, Al-Nahrain University, Baghdad, 10070, Iraq.*

Corresponding Author:

Ali Faris Al-Ghezi

Received: 07-01-2026
Revised: *28*-01-2026
Accepted: 12-02-2026
Published: 27-02-2026

Abstract: Schiff-Piece ligands were prepared from the reaction of thiadiazoles and triazoles with new aldehydes to obtain hetero-ligands, and some theoretical measurements were made using Docking to know their effect as inhibitors of bacteria, as well as some practical measurements were made at Al-Nahrain University, and it proved that these ligands can be used as inhibitors of bacteria.

Keywords: Synthesis; Schiff base; antagonists antibacteria.

INTRODUCTION

E. coli, a mostly facultative anaerobic Gram-negative bacteria, colonizes the digestive tract of newborn humans and aids in the maintenance of healthy intestinal homeostasis[1]. The three main categories of E. coli strains are (i) commensal strains found in the human and animal gut (lacking specialized virulence factors), (ii) intestinal pathogenic strains (diarrheagenic), and (iii) extraintestinal pathogenic E. coli (ExPEC) [2] . Despite not being connected to IBD, the diarrheagenic E. coli strains have been proven to clearly enhance intestinal inflammation and pathogenesis. Enteropathogenic E. coli (EPEC), Shiga toxin-producing E. coli (STEC), enterotoxigenic E. coli (ETEC), and enteroaggregative E. coli are the six well-known intestinal pathogenic E. coli varieties. coli, enteroinvasive E. coli, and diffusely adhering E. coli[3]. These E. coli strains can induce gastrointestinal illnesses such hemorrhagic colitis and self-limiting diarrhea[3].

Animals that are treated for infectious illnesses and prevented from getting them were shown to have antibiotic resistance[4]. Antimicrobial usage increases the prevalence of resistance in both pathogenic and endogenous bacteria, just as it does in humans[4]. Animals can transmit resistant germs to people via direct touch as well as through animal-derived foods. Multidrug resistance is characterized as the absence of inherent bacterial resistance to three or more antimicrobial groups[5]. Due to its outer membrane barrier, E. coli is inherently resistant to therapeutic concentrations of penicillin G, the first -lactam to be used in clinical practice. Additionally, E. coli is resistant to a variety of antibiotic classes with various modes of action[6, 7] . Molecular Docking

The development of molecular fusion began in the early 1980s. Once these programs became available, silico methodology (a term usually used for computer-conducted experiments)[8] .has been effectively used to discover several approved drugs, including HIV-1 inhibitors. The development of drugs has progressed

significantly and significantly since the use of (Silico methodology), which is currently the main approach in the discovery and development of drugs[9]. The primary purpose of molecular fusion is to attempt to determine the optimal position of an organic molecule (compound) in the protein environment. The design and development of drugs has made great progress with the help of computers, and the development of software and the availability of protein structures has helped a lot in the development and progress of this field[10].

The number of algorithms available for ligand-protein interactions is many and constantly increasing. This diversity in computational algorithms provides a large number of techniques to address modern drug design problems. Prediction of both the binding and affinity between ligand and protein is referred to as doking[11]. Understanding the structural determinants of the protein-ligand interaction and knowing the free energy (ΔG bind) are of great importance in the manufacture of pharmaceutical compounds, since it is a useful approach in the early stages of the drug discovery process, which helps to save time, effort and costs. Molecular docking is one of the most established methods for visualizing the interaction between a ligand and a protein and evaluating the binding mode of small molecules within the receptor binding site[11].

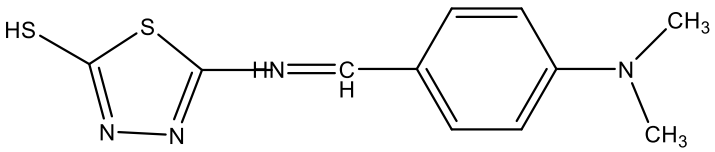

5-methyl-1,3,4-thiadiazole-2-thiol compound with 4-(iminomethyl)-*N*,*N*-dimethylaniline (1:1)
Chemical Formula: $C_{12}H_{16}N_4S_2$
Exact Mass: 280.08
Molecular Weight: 280.41
m/z: 280.08 (100.0%), 281.08 (13.0%), 282.08 (9.0%), 281.08 (1.6%), 281.08 (1.5%)
Elemental Analysis: C, 51.40; H, 5.75; N, 19.98; S, 22.87
[3]

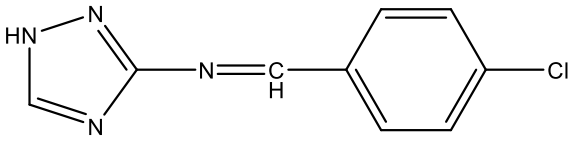

1-(4-chlorophenyl)-*N*-(1*H*-1,2,4-triazol-3-yl)methanimine
Chemical Formula: $C_9H_7ClN_4$
Exact Mass: 206.04
Molecular Weight: 206.63
m/z: 206.04 (100.0%), 208.03 (32.0%), 207.04 (9.7%), 209.04 (3.1%), 207.03 (1.5%)
Elemental Analysis: C, 52.31; H, 3.41; Cl, 17.16; N, 27.11
[4]

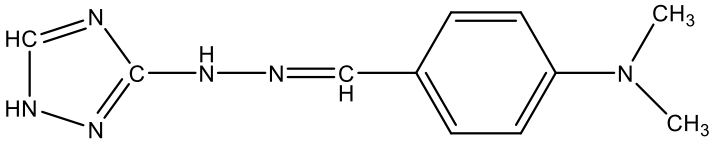

4-((2-(1*H*-1,2,4-triazol-3-yl)hydrazono)methyl)-*N*,*N*-dimethylaniline
Chemical Formula: $C_{11}H_{14}N_6$
Exact Mass: 230.13
Molecular Weight: 230.28
m/z: 230.13 (100.0%), 231.13 (11.9%), 231.13 (2.2%)
Elemental Analysis: C, 57.38; H, 6.13; N, 36.50

[7]

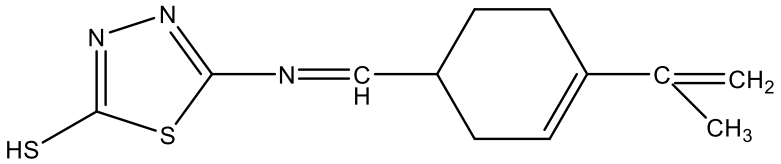

5-(((4-(prop-1-en-2-yl)cyclohex-3-en-1-yl)methylene)amino)-1,3,4-thiadiazole-2-thiol

Chemical Formula: $C_{12}H_{15}N_3S_2$

Exact Mass: 265.07

Molecular Weight: 265.39

m/z: 265.07 (100.0%), 266.07 (13.0%), 267.07 (4.5%), 267.07 (4.5%), 266.07 (1.6%), 268.07 (1.2%), 266.07 (1.1%)

Elemental Analysis: C, 54.31; H, 5.70; N, 15.83; S, 24.16

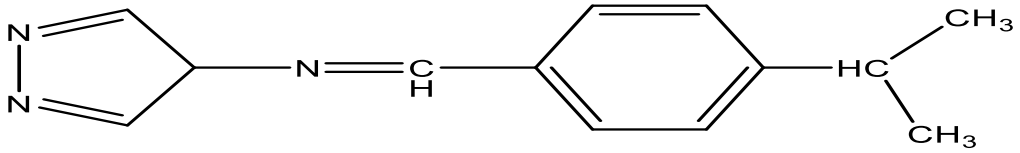

1-(4-isopropylphenyl)-*N*-(4*H*-pyrazol-4-yl)methanimine

Chemical Formula: $C_{13}H_{15}N_3$

Exact Mass: 213.13

Molecular Weight: 213.28

m/z: 213.13 (100.0%), 214.13 (14.1%), 214.12 (1.1%)

Elemental Analysis: C, 73.21; H, 7.09; N, 19.70

Nuclear Magnetic Resonance Spectra (1H-NMR)

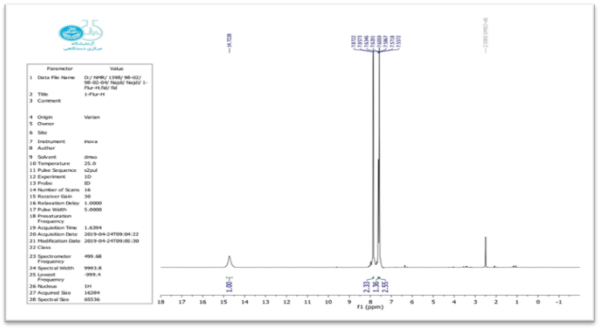

NMR spectra of free ligands were recorded in DMSO-2.51. H-NMR of L1 shows the signals (ppm) at (7.5572-7.8722), (4H, Ar-H), (1H- N=CH),) (1H, C-H-triazole), and (14.72) replace (1H, N-H). H-NMR of L2 shows the signals (ppm) at (7.5572- 7.8722), (4H, Ar-H), (1H- N=CH),) (1H, C-H-triazole), and (14.72) replace (1H, N-H) and showed (6H) at 3ppm replace to (CH3) 2-N. H-NMR of L3 shows the signals (ppm) at (7.5572- 7.8722), (4H, Ar-H), (1H,- N=CH),) (1H, C-H-triazole), and (14.72) replace (1H, N-H) and showed (6H) at1.5ppm replace to (CH3) 2-C and 1H at 5ppm replace to C .

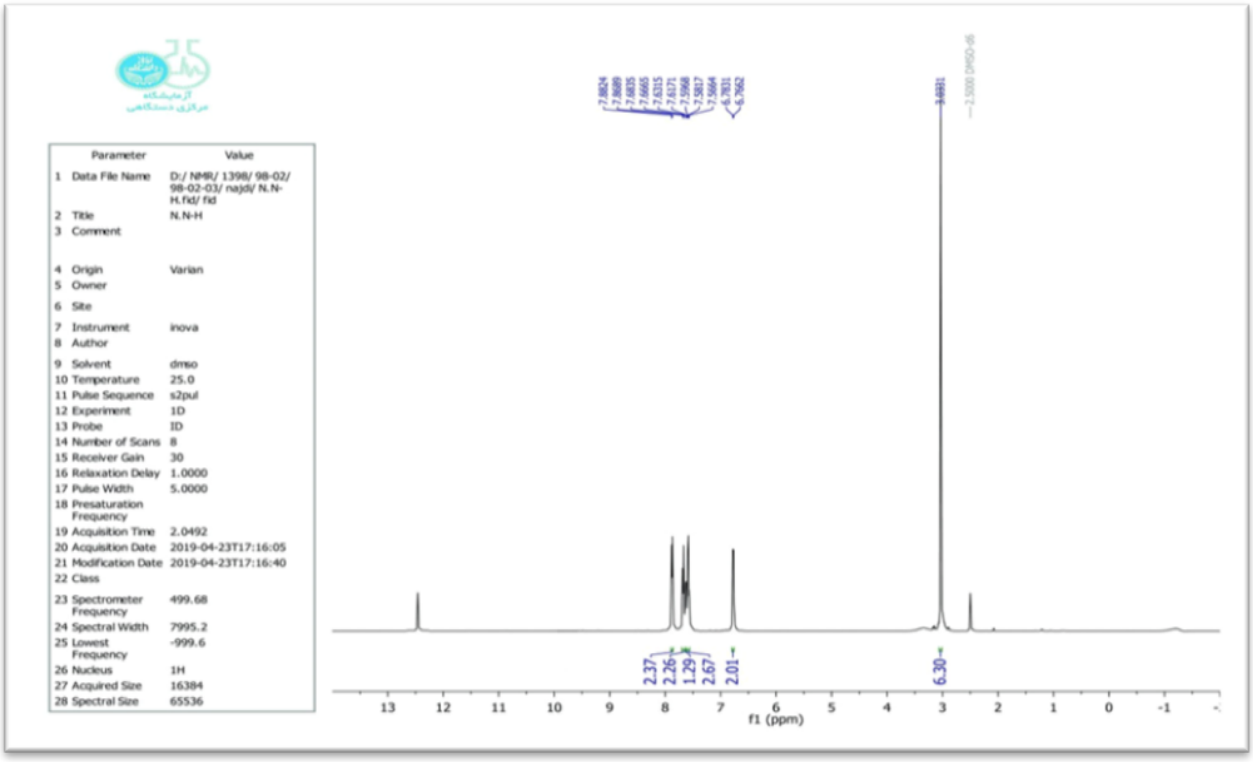

Figure (2) showed of H-NMR SPECTRUM Ligand6

Figure (3) showed of H-NMR SPECTRUM Ligand 7.

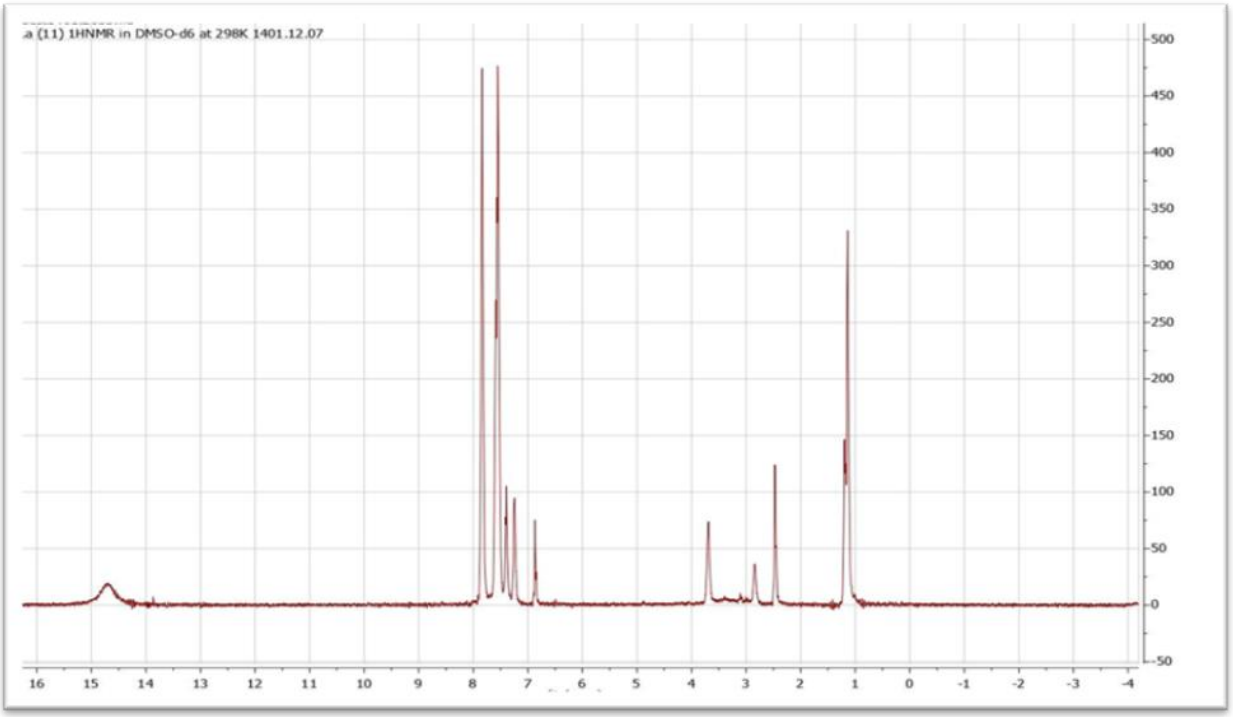

Figure (4) showed of H-NMR SPECTRUM Ligand9.

H NMR spectrum of ligand shows the signals (ppm) at 13 ppm(s-H),4H at 6.9-7.50ppm replace to (C-H) aromatice,1H at 8.71ppm N=C-H and 6H at 3ppm replace to N-(CH_3)2
HNMR of L2

H NMR spectrum of ligand shows the signals (ppm) at 13.23 ppm(s-H),3H at 1.79ppm replace to (-CH_3),1H at 8.10ppm N=C-H and 2H at 1.4-1.6 ppm replace to C=CH_2

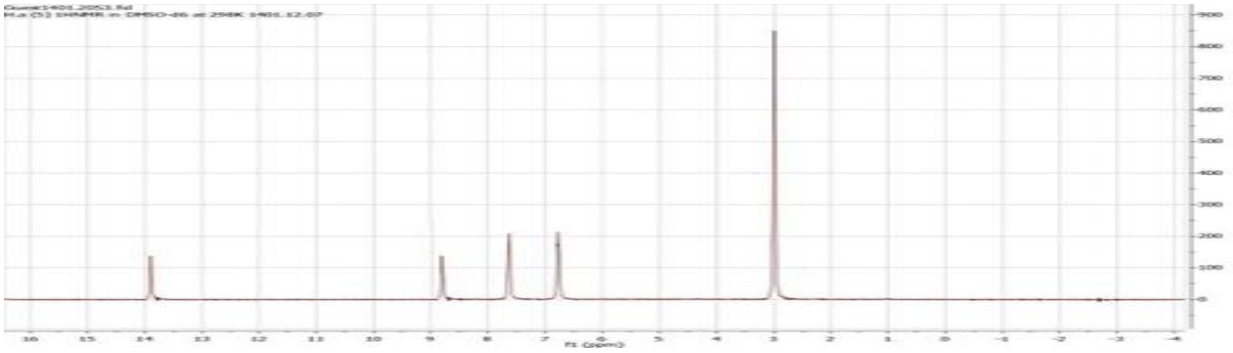

Fig (5) 1H-NMR spectra of the ligands (4).

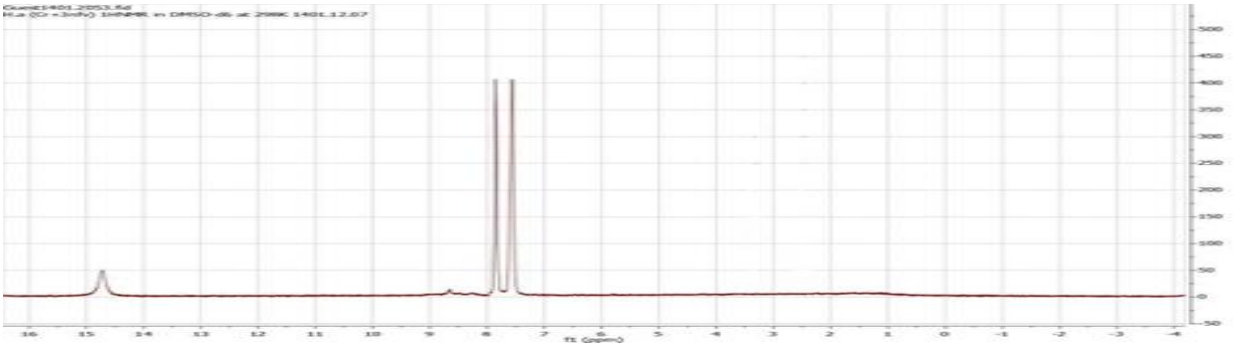

Fig (6) 1H-NMR spectra of The ligands(8). 1-2- FT-IR Spectra

Chemical Formula	υ (C-H)	υ (N-H)	υ (C=N) imine cm-1	C=C υ (C-Cl)	υ (N-C)
$C_9H_7CLN_4$	2984	2905	1618	825 -1735	1327

FT-IR of the complex ligand and its complexes was carried out from the KBr tweak to its ligand and Cs-I to the complexes. The Five bonding showed four main bands at (3100) cm-1, (2900) cm-1, (1608) cm-1, (825) cm-1, (1735) and (1327) which were attributed to (C-H), (υ H - N) imine, (C=N), (C-CL) (N-C), and movement ranges of the structure respectively, as shown in Table 1 .

Table 1. IR frequencies (cm-1) of the compound and their metal complexes.

Chemical Formula υ	υ (C-H)	υ (N-H)	υ (C=N) imine cm-1	υ (N-C)	C-CL
$C_{11}H_{13}N_5$	2900	3100.09	1608	1327	825

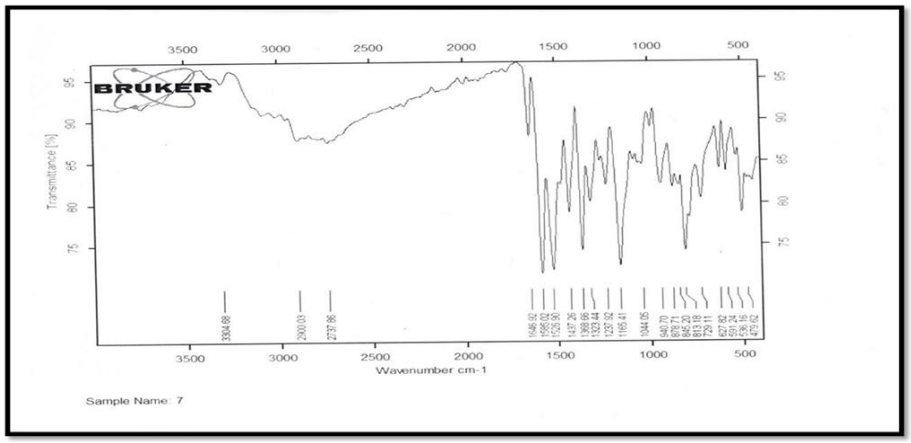

Figure (6)IR frequencies (cm-1) of the compound and their metal complexes of L7.

FT-IR of the complex ligand and its complexes was carried out from the KBr tweak to its ligand and Cs-I to the complexes. The sex bonding showed four main bands at (2984) cm-1, (2905) cm-1, (1618) cm-1, cm-1, (825) and (1735) which were attributed to (C-H), (υ H – N) imine, (C=N), (C-CL) (N-C), and movement ranges of the structure respectively, as shown below in Table 2 .

Table 2. IR frequencies (cm-1) of the compound and their metal complexes

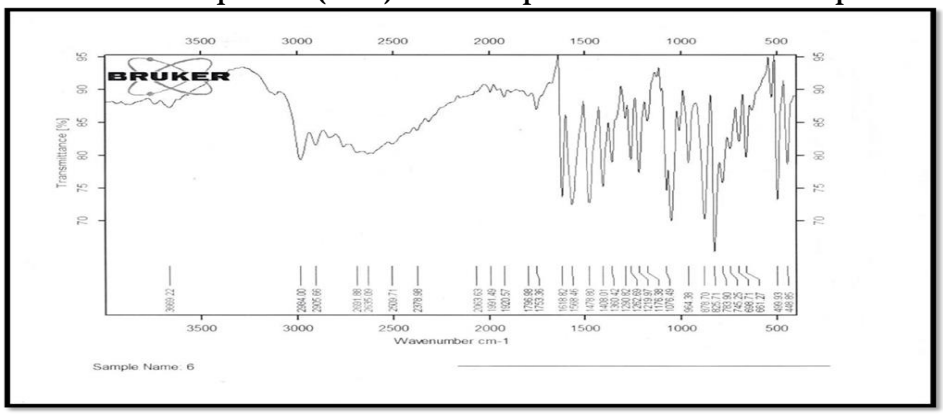

Figure (7)IR frequencies (cm-1) of the compound and their metal complexes of L1.

FT-IR of the complex ligand and its complexes was carried out from the KBr tweak to its ligand and Cs-I to the complexes. The sex bonding showed four main bands at (3237) cm-1, (2960) cm-1, (1617) cm-1, (1560) cm-1, (1478) and (1757) which were attributed to (C-H), (υ H = N) imine, (C=N), (C-CL) (N-C), and movement ranges of the structure respectively, as shown below in Table 3 .

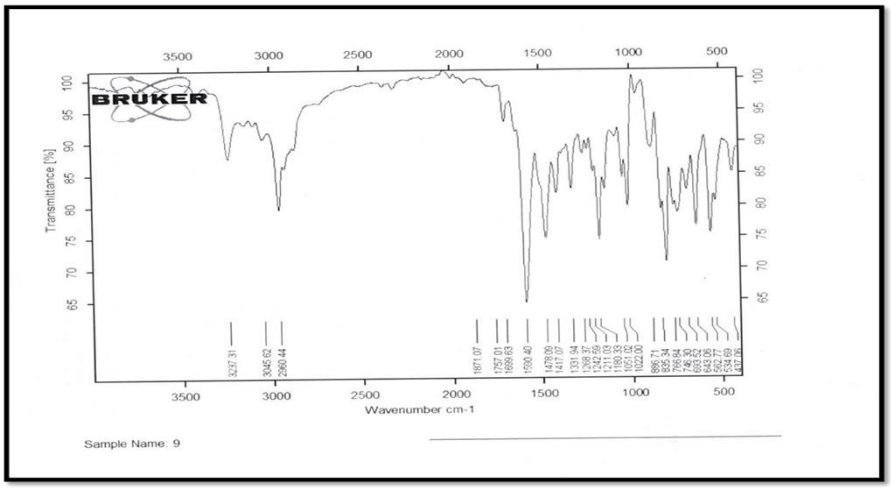

Table 3. IR frequencies (cm-1) of the compound and their metal complexes.

Figure (8)IR frequencies (cm-1) of the compound and their metal complexes of L3.

Chemical formula	υ (C-H)	υ (N-H)	υ (C=N) imine cm-1	Bending(C-H) C=C	υ bending (N-H)
$C_{12}H_{14}N_4$	2960	3237.31	1618	1735 825	1560

FT-IR Spectra

FT-IR Spectra FT-IR of the synthesized ligand were carried out KBr disc to ligand and CsI for complexes. The free ligand exhibited six major bands at (2924.09) cm-1, (1608) cm-1,(1481) cm-1,(1327) cm-1, which are attributable to (υ MN), (υ SH), (υ C=N) imine,(υ C-s-C) , (N-C), asy and structure movement bands respectively, as shown below (table1). New bands were formed attributed to the coordinated (CBr) bonds and appeared at the region (536,578,536)

cm-1. This indicates that the coordinate occurred through the (N)and (S) atoms (Table 2).

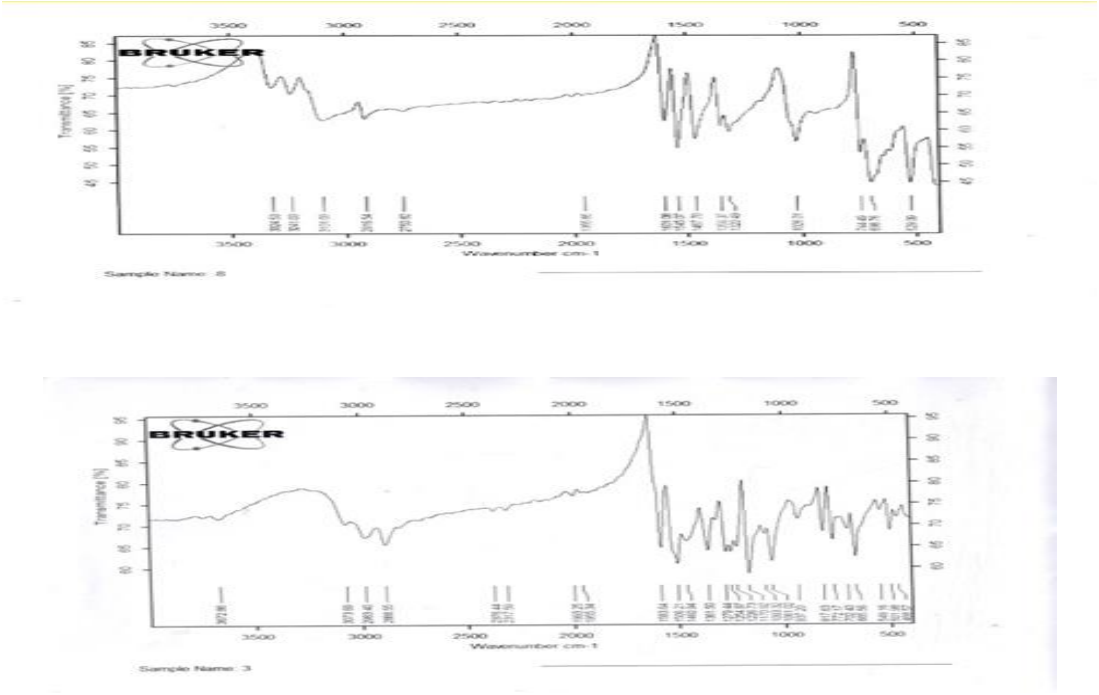

Fig (9) FT.IR spectrum of the ligands.

Table 3. IR frequencies (cm-1) of the compounds.

Chemical formula	υ (S-H)	υ (C-S-C)	υ (C=N) imine cm-1	υ (N-C)	C=C
$C_{11}H_{12}N_4S_2$	2960	1455	1608	1327	1668
$C_{12}H_{15}N_3S_2$	2967	1560	1560	1200	1690

Molecular docking

Molecular docking was conducted using AutoDock software . The 3D crystal structures of the E.coli protein (PDB ID: 2Q85) were retrieved from the Protein Data Bank. We used the AutoDock 4.2 to study the interactions between the protein and ligands. We submitted the PDB format of the protein and ligand in preparation for docking. Protein structures uploaded in PDB format to AutoDock are automatically cleaned with all water molecules removed and hydrogen polar atoms added to the structure using MGL Tools. After that, the active sites in the crystal structures of the protein . To visualize the molecular structures, we employed Discovery Studio 2021 Client[12].

Molecular docking analysis

The interaction between ligand 11 and E.coli was studied using AutoDock . The complex with least binding affinity −9.11 kcal/mol was selected for protein ligand interaction study. Fig. 1 showed the interaction between recombinant compound 11 with E.coli . The amino acids involved in catalytic activity of E.coli were determined through docking. Our docking observation suggested the involvement of TYR-125A, GLY-126A and TYR-190A residues in the formation of recombinant compound11-E.coli complex with bond length of 2.20, 2.10 and 1.77 Ao respectively. These docking results suggests that, TYR-125A, GLY-126A, and TYR-190A are critical for compound11-E.coli interaction. The surrounding hydrophobic amino acids further stabilized the complex and enhanced enzyme activity and thermo stability [13] .

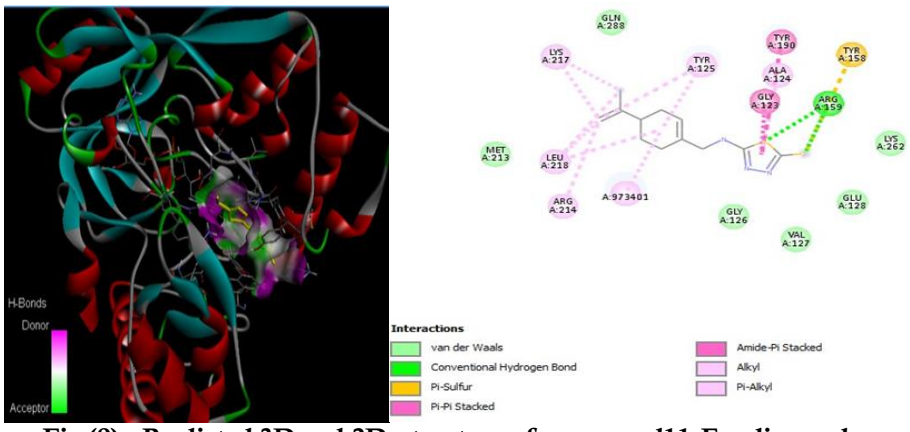

Fig (9) : Predicted 3D and 2D structure of compound11-E.coli complex

Molecular docking

Molecular docking was conducted using AutoDock software. The 3D crystal structures of the E.coli protein (PDB ID: 2Q85) were retrieved from the Protein Data Bank. We used AutoDock 4.2 to study the interactions between the protein and ligands. We submitted the PDB format of the protein and ligand in preparation for docking. Protein structures uploaded in PDB format to AutoDock are automatically cleaned with all water molecules removed and hydrogen polar atoms added to the structure using MGL Tools. After that, the active sites in the crystal structures of the protein. To visualize the molecular structures, we employed Discovery Studio 2021 Client [12, 13-19].

Molecular docking analysis

The molecular fusion results for the compounds were as shown in Table 4

Table 4 : Molecular docking results for the compounds under study

Compound NO	Lowest Binding Energy	Run
3	-7.81	21
9	-6.68	24
8	-9.11	22
7	-7.07	37
6	-8.88	29

The hydrogen bonds of the studied compounds were as shown in Table 5

Table 5: Hydrogen Bonds and Amino acids and bond Length

Compound NO	AA	Distance H-A
7	GLN168A ARG327A ARG327A	2.90A 2.15A 2.83A
3	TYR125A	2.40A
9	VAL43A ILE45A GLN168A PHE171A	1.93A 2.92A 2.19A 3.35A
8	TYR125A GLY126A TYR190A	2.20 2.10 1.77

As that Hydrophobic Interactions and π-Stacking were as shown in Table 6.

Table 6: Hydrophobic Interactions and π-Stacking

Compound NO	Hydrophobic Interactions		π-Stacking	
	AA	Distance	AA	Distance
7	ILE 45A	3.68		

3	TYR 190A	3.47	TYR 125A	4.33
	LEU 218A	3.21		
	LEU 218A	3.39		
9	LEU 44A	3.68		
	ILE 119A	3.99		
	ILE 119A	3.90		
	GLN 168A	3.97		
	GLU 334A	3.32		
8	TYR 125A	3.91		
	TYR 125A	3.68		
	TYR 190A	3.38		
	LYS 217A	3.66		
	LYS 217A	3.80		
	LEU 218A	3.14		

The associations between the compounds and the protein are shown as in table 7.

Table 7: Bonding of compounds with the target proton in 2D and 3D

Compound NO.	2D	3D
7	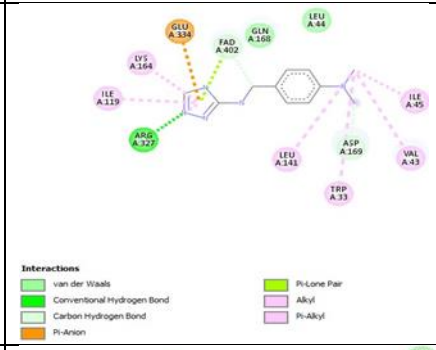	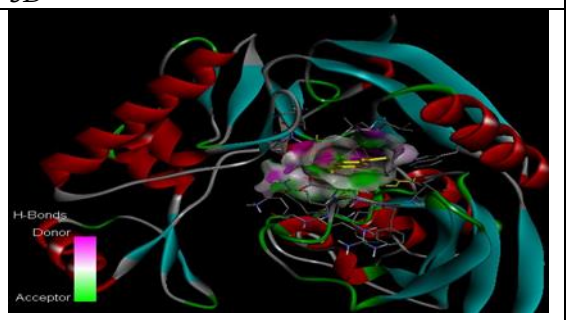
3	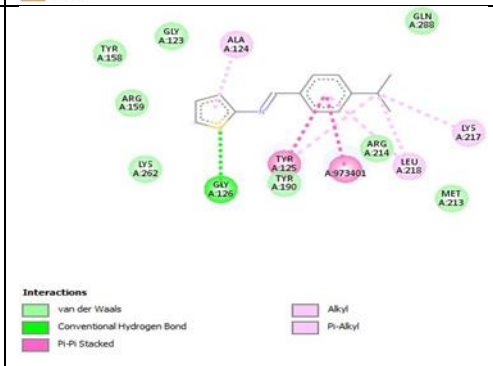	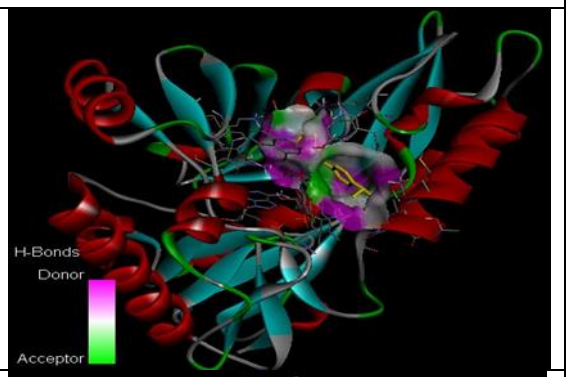
9	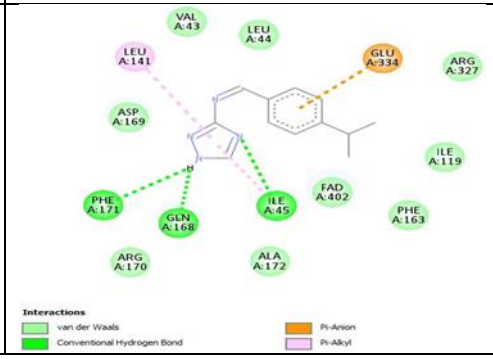	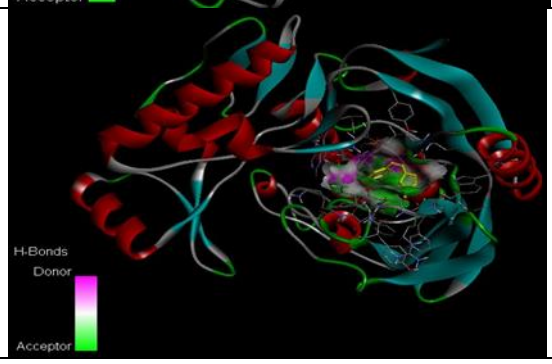

The interaction between ligand 11 and E.coli was studied using AutoDock . The complex with least binding affinity −9.11 kcal/mol was selected for protein ligand interaction study. Fig. 1 showed the interaction between recombinant compound 8 with E.coli . The amino acids involved in catalytic activity of E.coli were determined through docking. Our docking observation suggested the involvement of TYR-125A, GLY-126A and TYR-190A residues in the formation of recombinant compound11-E.coli complex with bond length of 2.20, 2.10 and 1.77 Ao respectively.

These docking results suggests that, TYR-125A, GLY-126A, and TYR-190A are critical for compound11-E.coli interaction. The surrounding hydrophobic amino acids further stabilized the complex and enhanced enzyme activity and thermo stability.

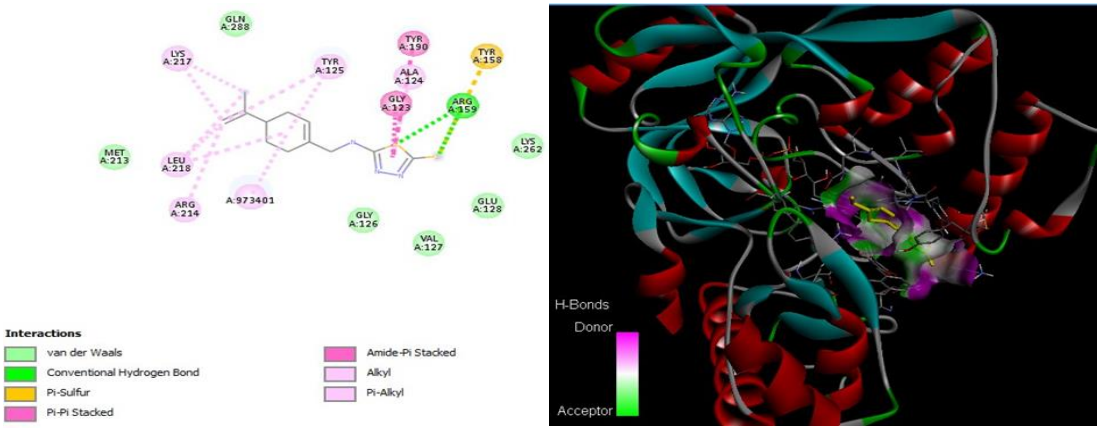

Fig (11): Predicted 3D and 2D structure of compound8-E.coli complex

Method for preparing a standard solution saturated with the prepared materials

1-A measured amount of each compound was taken at a concentration of 0.05M, and the weight was calculated according to the law of molar concentration.

2- Each ligand was dissolved in a 20ml conical boat with DMSO solvent, and the volume was completed to the end.

3- Tests of the effectiveness of these substances against bacteria were carried out at the Biotechnology Center, Al-Nahrain University

Table It shows the use of weights and concentrations of solutions for each ligand

no	mass	Mol/L
L3	0.264g	0.05
L4	0.206g	0.05
L6	0.206g	0.05
L7	0.215g	0.05
L8	0.214g	0.05
L9	0.244g	0.05

Comp. No.	***Anti- bacterial Activity***
	E.coli
3	+
4	+
6	+
7	+
8	++
9	++

The antibacterial activity of the prepared compounds was studied against a type of Escherichia coli (Gram-negative bacteria) as shown in Table No. (8): -

Table 9: Antibacterial activity test data (inhibition area in mm) for the prepared compounds.

(+++) ; high active – inhibition zone = 20 mm , (++) :moderate active - inhibition zone =14-20 mm , (+) : slighly active - inhibition zone = 9-14 mm , (-) : inactive

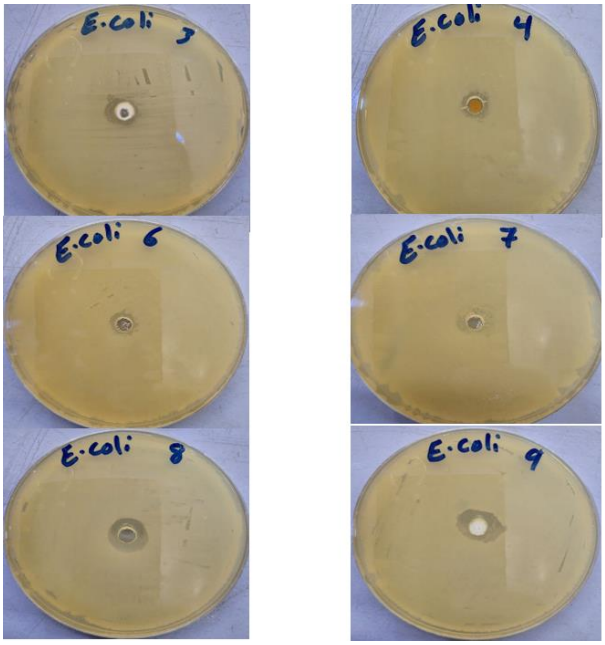

Figure (12):- The biological effect of the compounds on Escherichia coli bacteria

REFERENCES

1. Kelly, D., T. King, and R. Aminov. "Importance of Microbial Colonization of the Gut in Early Life to the Development of Immunity." *Mutation Research/Fundamental and Molecular Mechanisms of Mutagenesis*, vol. 622, no. 1–2, 2007, pp. 58–69.
2. Russo, T. A., and J. R. Johnson. "Proposal for a New Inclusive Designation for Extraintestinal Pathogenic Isolates of Escherichia coli: ExPEC." *The Journal of Infectious Diseases*, vol. 181, no. 5, 2000, pp. 1753–1754.
3. Kaper, J. B., J. P. Nataro, and H. L. T. Mobley. "Pathogenic Escherichia coli." *Nature Reviews Microbiology*, vol. 2, no. 2, 2004, pp. 123–140.
4. Szmolka, A., and B. Nagy. "Multidrug Resistant Commensal Escherichia coli in Animals and Its Impact for Public Health." *Frontiers in Microbiology*, vol. 4, 2013, p. 258.
5. Magiorakos, A.-P., et al. "Multidrug-Resistant, Extensively Drug-Resistant and Pandrug-Resistant Bacteria: An International Expert Proposal for Interim Standard Definitions for Acquired Resistance." *Clinical Microbiology and Infection*, vol. 18, no. 3, 2012, pp. 268–281.
6. Johnson, T. J., et al. "Associations between Multidrug Resistance, Plasmid Content, and Virulence Potential among Extraintestinal Pathogenic and Commensal Escherichia coli from Humans and Poultry." *Foodborne Pathogens and Disease*, vol. 9, no. 1, 2012, pp. 37–46.
7. Erb, A., et al. "Prevalence of Antibiotic Resistance in Escherichia coli: Overview of Geographical, Temporal, and Methodological Variations." *European Journal of Clinical Microbiology & Infectious Diseases*, vol. 26, 2007, pp. 83–90.
8. Ekins, S., J. Mestres, and B. Testa. "In Silico Pharmacology for Drug Discovery: Methods for Virtual Ligand Screening and Profiling." *British Journal of Pharmacology*, vol. 152, no. 1, 2007, pp. 9–20.
9. Muegge, I., A. Bergner, and J. M. Kriegl. "Computer-Aided Drug Design at Boehringer Ingelheim." *Journal of Computer-Aided Molecular Design*, vol. 31, no. 3, 2017, pp. 275–285.
10. Potemkin, V., and M. Grishina. "Grid-Based Technologies for In Silico Screening and Drug Design." *Current Medicinal Chemistry*, vol. 25, no. 29, 2018, pp. 3526–3537.
11. Lybrand, T. P. "Ligand–Protein Docking and Rational Drug Design." *Current Opinion in Structural Biology*, vol. 5, no. 2, 1995, pp. 224–228.
12. Cosconati, S., et al. "Virtual Screening with AutoDock: Theory and Practice." *Expert Opinion on Drug Discovery*, vol. 5, no. 6, 2010, pp. 597–607.
13. Forli, S., et al. "Computational Protein–Ligand Docking and Virtual Drug Screening with the AutoDock Suite." *Nature Protocols*, vol. 11, no. 5, 2016, pp. 905–919.
14. Bashar, Bashar S., et al. "Application of Novel Fe_3O_4/Zn-Metal Organic Framework Magnetic Nanostructures as an Antimicrobial Agent and Magnetic Nanocatalyst in the Synthesis of Heterocyclic Compounds." *Frontiers in Chemistry*, vol. 10, 2022, article 1014731.

15. Althomali, Raed H., et al. "A Novel Pt-Free Counter Electrode Based on $MoSe_2$ for Cost Effective Dye-Sensitized Solar Cells (DSSCs): Effect of Ni Doping." *Journal of Physics and Chemistry of Solids*, vol. 182, 2023, article 111597.
16. Al-dolaimy, F., et al. "Incorporating of Cobalt into UiO-67 Metal–Organic Framework for Catalysis CO_2 Transformations: An Efficient Bi-Functional Approach for CO_2 Insertion and Photocatalytic Reduction." *Journal of Inorganic and Organometallic Polymers and Materials*, 2023, doi:10.1007/s10904-023-02860-0.
17. Al-Hawary, S. I. S., et al. "Tunneling Induced Swapping of Orbital Angular Momentum in a Quantum Dot Molecule." *Laser Physics*, vol. 33, no. 9, 2023, article 096001.
18. Zaman, Gaffar Sarwar, et al. "Electrochemical Determination of Zearalenone in Agricultural Food Samples Using a Flower-Like Nanocomposite-Modified Electrode." *Materials Chemistry and Physics*, vol. 305, 2023, article 127986.
19. Khursheed, Muzammil, et al. "Methanol Extract of Iraqi Kurdistan Region Daphne mucronata as a Potent Source of Antioxidant, Antimicrobial, and Anticancer Agents for the Synthesis of Novel and Bioactive Polyvinylpyrrolidone Nanofibers." *Frontiers in Chemistry*, 2023, doi:10.3389/fchem.2023.1287870.

